ACS APPLIED MATERIALS & INTERFACES

Research Article

www.acsami.org

Pre-Lithiation of $Li(Ni_{1-x-y}Mn_xCo_y)O_2$ Materials Enabling Enhancement of Performance for Li-Ion Battery

Zhongzhen Wu,[†,#] Shunping Ji,[†,#] Zongxiang Hu,[†,#] Jiaxin Zheng,[†] Shu Xiao,[†] Yuan Lin,[†] Kang Xu,[‡] Khalil Amine,[§] and Feng Pan*[,†]

[†]School of Advanced Materials, Peking University Shenzhen Graduate School, Shenzhen 518055, China

[‡]U.S. Army Research Laboratory, Adelphi, Maryland 20783, United States

[§]Electrochemical Technology Program, Chemical Sciences and Engineering Division, Argonne National Laboratory, Argonne, Illinois 60439, United States

Supporting Information

ABSTRACT: Transition metal oxide materials $Li(Ni_xMn_yCo_z)O_2$ (NMC*xyz*) based on layered structure are potential cathode candidates for automotive Li-ion batteries because of their high specific capacities and operating potentials. However, the actual usable capacity, cycling stability, and first-cycle Coulombic efficiency remain far from practical. Previously, we reported a combined strategy consisting of depolarization with embedded carbon nanotube (CNT) and activation through pre-lithiation of the NMC host, which significantly improved the reversible capacity and cycling stability of NMC532-based material. In the present work we attempt to understand how pre-lithiation leads to these improvements on an atomic level with experimental investigation and ab initio calculations. By lithiating a series of NMC materials with varying chemical compositions prepared via a conventional approach, we identified the Ni in the NMC lattice as the component responsible for accommodating a double-layered Li structure. Specifically, much better improvements in the cycling stability and capacity can be achieved with the NMC lattices populated with Ni^{3+} than those populated with only Ni^{2+}. Using the XRD we also found that the emergence of a double-layer Li structure is not only reversible during the pre-lithiation and the following delithiation, but also stable against elevated temperatures up to 320 °C. These new findings regarding the mechanism of pre-lithiation as well as how it affects the reversibility and stability of NMC-based cathode materials prepared by the conventional slurry approach will promote the possibility of their application in the future battery industry.

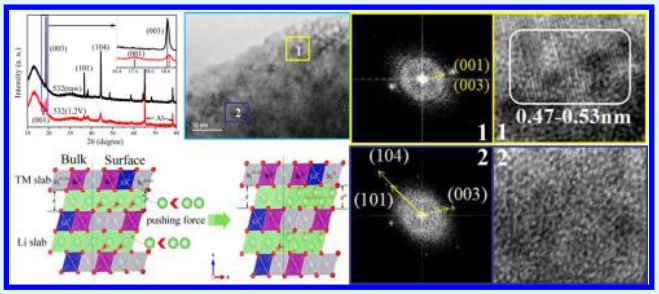

KEYWORDS: *pre-lithiation, $Li(Ni_xMn_yCo_z)O_2$ (NMCxyz), ab initio calculations, double-layered Li structure, cycling stability and capacity*

INTRODUCTION

As Tesla motors continue to sweep the world, layered transition metal oxide ($Li(Ni_xMn_yCo_{1-x-y})O_2$, or NMC) materials with both higher voltage and higher capacity are expected to replace both $LiCoO_2$ and $LiFePO_4$ as the cathode of choice in the near future. However, despite the promised theoretical value (~280 mAh/g), the capacity that can be reversibly accessed (~170 mAh/g) is always much lower and fades faster than desired.[1,2] The capacity decay in the long term cycling has been attributed to diversified factors including Mn(II)-dissolution from NMC lattice, the poisoning of anode interphase by Mn(II) species,[3] the simultaneous phase-transformation from layered to spinel near the surface of NMC particles,[4] as well as irreversible loss of active ingredients caused by the side reaction between transition metal elements and electrolyte near the particle surfaces.[5]

In order to improve the performance of NMC-based materials, our previous efforts have been dedicated to resolving these issues either by depolarizing the particle with carbon nanotubes (CNT) embedded therein,[6] or by pre-lithiating the cathode materials at low potentials so that an interphase chemically similar to that formed on an anode surface would form and protect cathode particles.[7] The latter strategy has been proven especially effective for the NMC532 composite depolarized by CNT, in which not only the formed interphase suppressed the Mn(II)-dissolution and ensure better cycling performances, but also the lithiation process induces a double Li structure near the surface of NMC particles and introduces additional capacity. In this work, employing electrochemical, spectroscopic, and computational means we attempt to understand how pre-lithiation enables the NMC lattice to accommodate such excess Li substructure. By systematically

Received: March 28, 2016
Accepted: May 30, 2016
Published: May 30, 2016

DOI: 10.1021/acsami.6b03730
ACS Appl. Mater. Interfaces 2016, 8, 15361−15368

examining how different NMC materials respond to a pre-lithiation process, we establish a precise correlation between the valence state of Ni in NMC and the extent by which pre-lithiation occurs. In particular, NMC materials rich in Ni^{3+} exhibit apparent structural transformation induced by pre-lithiation, accompanied by significant performance enhancement as compared with those populated with only Ni^{2+}. The electrochemical reversibility of double-layer Li structure as well as its thermal stability are also investigated. Ab initio calculations are used to investigate how the pre-lithiated NMC group stores excessive two-layer Li with the different delithiation and lithiaton voltages.

EXPERIMENTAL SECTION

The NMC series materials (NMC811, NMC71515, NMC622, NMC532, NMC552, NMC442, and NMC333) were purchased from Shenzhen Tianjiao Technology Co., Ltd. All cathode samples in the batteries were prepared by conventional slurry method. The mixed ratio of NCM powders, carbon black, and PVDF was 75:15:10. All the cell tests were done with a 2032 coin-cell using Li metal as the anode. The electrolyte is purchased from Shenzhen CAPCHEM Technology Co. Ltd. (LBC3045M38). All the operations were conducted in an argon-filled glovebox. For the pre-lithiation, the cell was discharged to the voltage requested in this work first before the conventional State of Charge (SOC) at current density of 0.1 C. Then, the cell was cycled between 3.0 and 4.5 V at current density of 2 C and 5 C at 25 °C.

Cycled NCM serial cathodes were harvested from the cells for characterization by TEM, SEM, and XRD analyses. Before the test, the electrodes were immersed in dimethyl carbonate (DMC) for 24 h and then rinsed with fresh DMC three times before drying under vacuum. The morphology of the purchased powder was observed by SEM (JSM-6340F, JEOL). The electron diffraction and the high-resolution lattice structure images of the prepared samples were observed by TEM (FEI Tecnai G2 F30). The structure of the NCM serial materials before and after cycling was characterized on a Bruker D8 Advance XRD using Cu Kα radiation (λ = 1.5418 Å). The XRD patterns were obtained with a scan speed of 0.02° per step over a 2θ range of 10−80°.

In order to calculate the excess Li intercalated into the surface of the NMC serial cathode materials for lithium ion batteries, we build a supercell comprising 4 × 4 unit cell containing 30 formula units with the prototypical $R\bar{3}$ m layer structure. All calculations are performed using the plane-wave projector-augmented wave method with an energy cutoff of 400 eV,[8,9] as implemented in the Vienna ab initio simulation package (VASP).[10,11] The Perdew−Burke−Ernzerhof (PBE) form of generalized gradient approximation (GGA) is chosen as the exchange-correlation potential.[12] The PBE+U approach is employed to take account of the strong on-site Coulomb interaction (U) presented in the localized 3d electrons of Mn, Co, and Ni, with the U values set to 3.9, 3.32, and 6.2 eV for them, respectively.[13] To obtain reliable optimized structures and the total energy, all the atomic positions and cell parameters are fully relaxed. The maximum residual force is less than 0.02 eV/Å and energies are converged to within 1 × 10^{-4} eV per atom, and the k-point mesh is set to 4 × 2 × 4 for 532 and 4 × 2 × 2 for 622, 71515, 811.

RESULTS AND DISCUSSION

The compositions of all NMC series materials are determined by Inductively Coupled Plasma-Atomic Emission Spectroscopy (ICP-AES), as shown in Table 1. In all cases each element was found in comparable proportions with its intended composition. A slight deficiency of Li was observed in NMC71515 and NMC811, but an opposite trend is found in all other materials. Under SEM, the NMC particles are found to consist of 5−10 μm spherical secondary particles aggregated by submicron-sized primary particles, which are distributed in a narrow range of 300−500 nm, as shown in Supporting Information Figure S1.

Table 1. Compositions of the NMC Series Materials Detected by ICP-AES

material	Li [at%]	Ni [at%]	Mn [at%]	Co [at%]
811	0.94	0.79	0.11	0.10
71515	0.95	0.69	0.16	0.15
622	1.04	0.6	0.21	0.23
532	1.02	0.5	0.29	0.2
552	1.04	0.43	0.42	0.17
442	1.06	0.4	0.39	0.2
333	1.07	0.33	0.35	0.32

Before pre-lithiation, the voltage profiles of the NMC series materials during the first charging process between 3.0 and 4.5 V are shown in Figure 1 along with corresponding cyclic voltammograms. The polarization initially intensifies with the Ni content until 42%, and then the trend reverses. Compared to the voltage plateau of the redox reaction at 3.8 V, NMC71515 exhibits the minimum polarization, which increases successively with NMC622, NMC532, and NMC552.

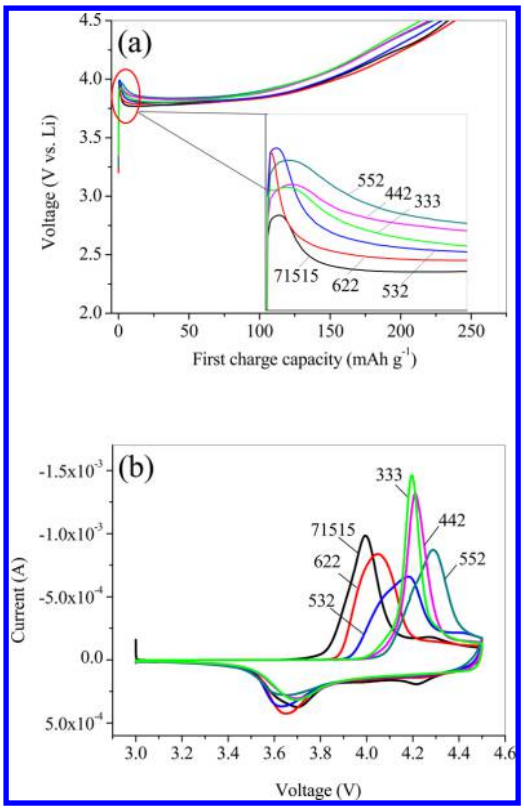

Figure 1. Voltage polarization in the NMC series materials during the first charging process without pre-lithiation: (a) voltage profiles and (b) cyclic voltammograms.

After pre-lithiation, all the materials are effectively depolarized, as evidenced by the voltage profiles shown in Figure 2 for the materials during the lithiation and charging processes immediately afterwards. Voltage plateaus are observed in the NMC71515, NMC622, and NMC532 in the pre-lithiation at 1.2 V, while no such plateau is observed for the other three. The depolarization degree seems to correspond well with the presence of long lithiation plateaus: while high polarization still remains with those NMC materials that failed to be effectively

DOI: 10.1021/acsami.6b03730
ACS Appl. Mater. Interfaces 2016, 8, 15361−15368

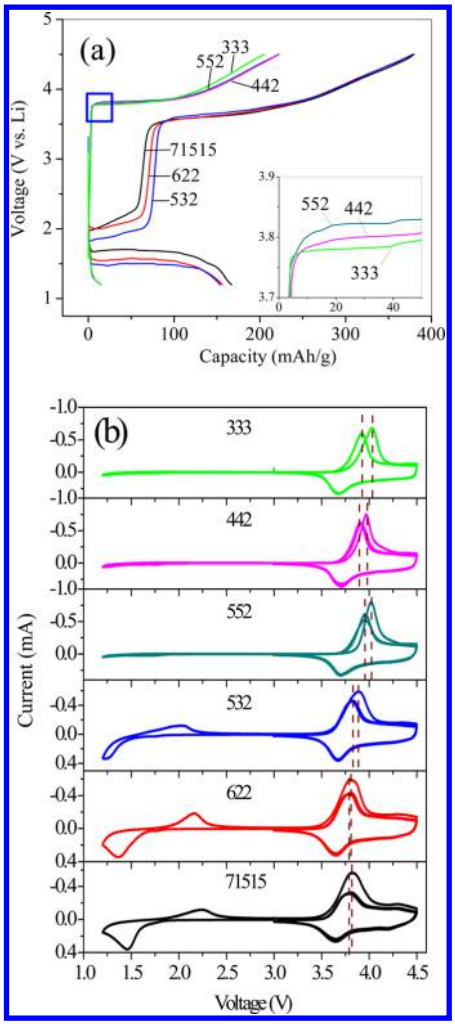

Figure 2. (a) Voltage profiles of NMC series materials during the pre-lithiation (~1.2 V) and then in the first charging process immediately thereafter; (b) cyclic voltammograms of the pre-lithiated NMC series materials in the first charge/discharge cycle.

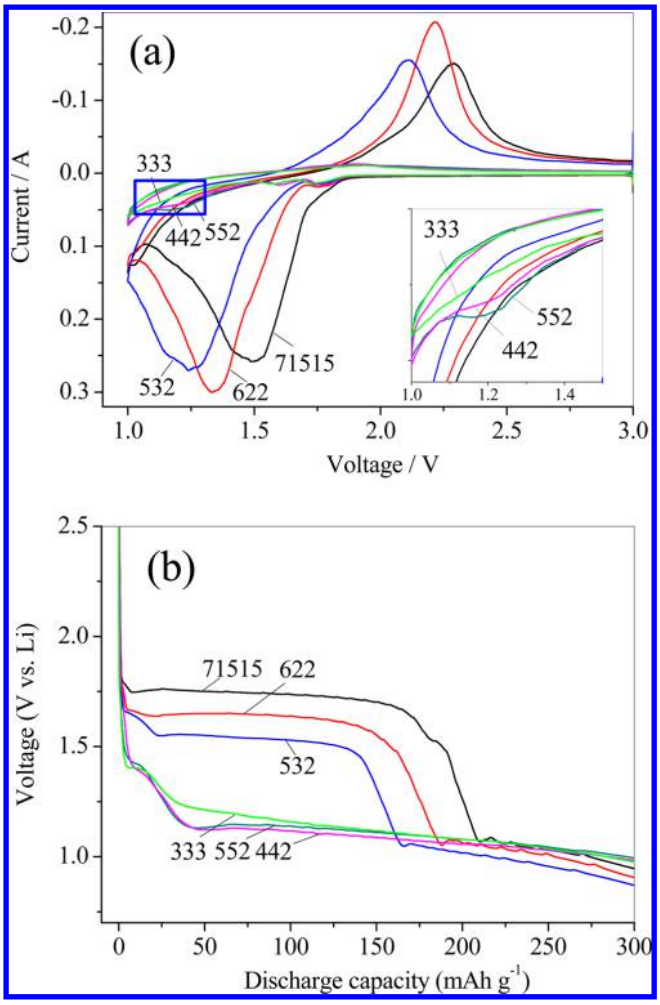

Figure 3. Electrochemical performances of the $Li(Ni_{1-x-y}Mn_xCo_y)O_2$ materials during the pre-lithiation and the subsequent cycles between 3.0 and 1.0 V: (a) cyclic voltammograms and (b) voltage profiles.

lithiated, significant depolarization is realized for those that showed lithiation plateaus. Thus, we tentatively divide all the NMC materials examined in this work into two groups according to their distinctly different pre-lithiation behaviors at 1.2 V: NMC71515, NMC622, and NMC532, which allow significant lithiation and are thus significantly depolarized; and NMC552, NMC442, and NMC333, which show limited lithiation and depolarization.

A deeper pre-lithiation down to 1.0 V is also conducted, whose CV curves and voltage profiles are shown in Figure 3. Similar correlations between pre-lithiation and voltage profiles are observed, i.e., for those exhibiting lithiation plateaus, both depolarization and lithiation extent decrease with Ni content following the order of NMC71515, NMC622, and NMC532. When pre-lithiation voltage is reduced down to 1.0 V, another voltage platform becomes visible in all the NMC materials, which reflects the destruction of the NMC lattice by overly excessive Li intercalation.[14,15]

In order to shed more light on the mechanism of NMC lithiation at the atomic level, on the voltage profile of NMC532 material we selected eight points, where the compositions and the phase structures are individually examined, as shown in Figure 4. Based on post-mortem analysis by ICP-AES, the Li contents in the NMC532 cathode materials continuously increase with the discharge voltage in the pre-lithiation. At 1.2 V, about 66% more Li^+ is already inserted in the NMC532 lattice. Interestingly, while most of the excess Li^+ can be reversibly removed in the following charging process at low potentials below 2.5 V, 23% would remain in NMC532 when the material is charged to the original open circuit voltage. In other words, around 23% excess Li^+ will remain in the NMC lattice and contribute to the reversible capacity that can be accessed during normal charge/discharge cycles between 3.0 and 4.5 V.

A similar conclusion can be drawn from XRD patterns from those points on the voltage profile, as shown in Figure 4c,d. The (001) peak which stands for double layered Li structure can be observed when the discharge voltage is below 1.5 V,[15] as happened in the NMC532 lattice in our previous work.[7] The double layered Li structure serves as a reversible Li source when the battery is charged back to 4.0 V. Meanwhile, the (003) peak decreases at the increasing discharge depth because of the insertion of excess Li^+. NMC532 particles were also examined after pre-lithiation using high-resolution TEM images and XRD, shown in Figure 5, which also confirm the generation of double-layered Li structure by pre-lithiation. The (001) plane can be observed at certain locations, such as region 1 in Figure 5b. The *d*-spacing revealed by high-resolution TEM in Figure

DOI: 10.1021/acsami.6b03730
ACS Appl. Mater. Interfaces 2016, 8, 15361−15368

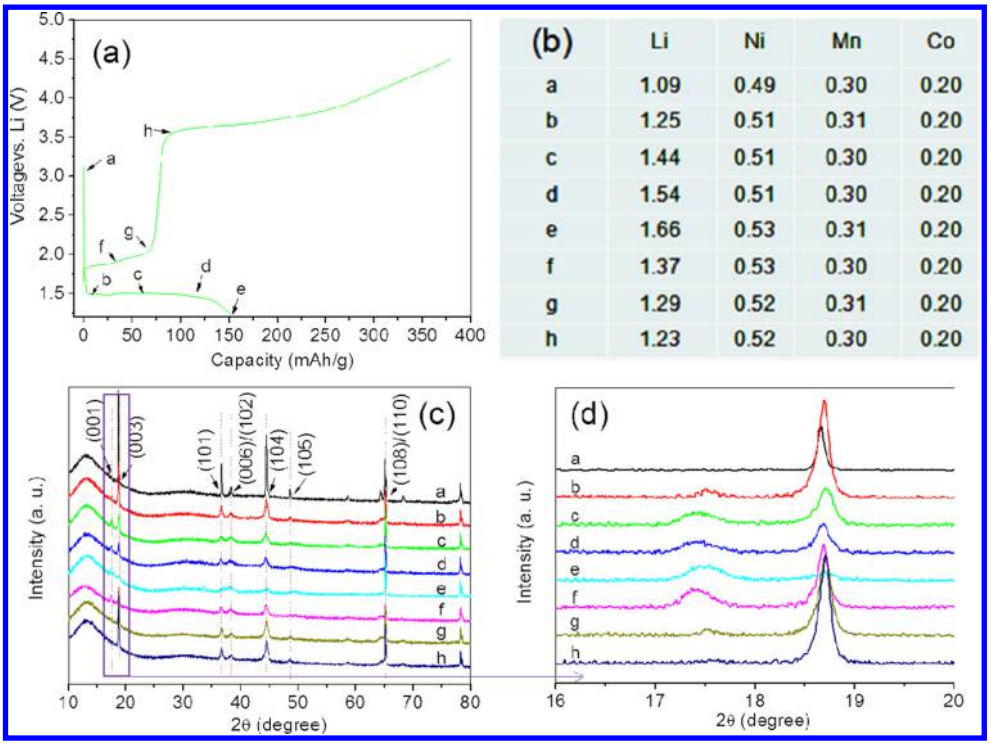

(b)	Li	Ni	Mn	Co
a	1.09	0.49	0.30	0.20
b	1.25	0.51	0.31	0.20
c	1.44	0.51	0.30	0.20
d	1.54	0.51	0.30	0.20
e	1.66	0.53	0.31	0.20
f	1.37	0.53	0.30	0.20
g	1.29	0.52	0.31	0.20
h	1.23	0.52	0.30	0.20

Figure 4. Characterizations of NMC532 materials at different charge/discharge states as labeled on the voltage profiles: (a) selected charge/discharge states, (b) composition determined by ICP-AES at the corresponding charge/discharge states, (c) XRD patterns at the corresponding charge/discharge states, and (d) the magnified view of the marked section in (c).

5e lies in the range of 0.47−0.53 nm, which is much larger than that of NMC532 populated with single-layered Li (0.47 nm).[16,17] This might be the result of the interlayer expansion induced by excess Li insertion during the pre-lithiation.[18] However, not all Li locations in this layer are occupied, as shown in Figure 5d−g. For example, no (001) peak is discovered in point 2 in Figure 5b, suggesting the NMC material in this location region still retains the single-layer Li structure, with *d*-spacing of 0.47 nm.

In sharp contrast to NMC71515, NMC622, and NMC532, no (001) peak can be observed at all in the second group of NMC materials, NMC552, NMC442, and NMC333, even after they are pre-lithiated to 1.2 V as shown in Figures S2−S6. Thus, an excellent agreement exists between the structural evolution and electrochemical behavior at lithiation potential, and clearly defines two distinctly different groups of NMC materials. Actually, the main difference between the two groups is the content of Ni and Mn and the induced valence state of Ni in the NMC lattice. The first group, represented by NMC552, NMC442, and NMC333, contain Ni and Mn at 1:1 ratio, indicating that the valence of Ni is 2 and no Ni^{3+} should be present. In the other group, NMC71515, NMC622, and NMC532, however, Ni is in much higher percentage as compared with Mn, suggesting that two valence states of Ni (Ni^{2+} and Ni^{3+}) should coexist.[19] We believe that it was because of the presence of Ni^{3+} that the NMC materials can be further reduced by the insertion of excess Li^+ during the pre-lithiation, accompanied by the reduction of Ni^{3+} into Ni^{2+}. Naturally, when Ni^{3+} is absent, excess Li^+ cannot be accommodated unless Ni^{2+} can be further reduced into metallic Ni, which involves a much higher energy barrier and requires much lower potential to proceed. We performed ab initio calculations for the pre-lithiatied group, NMC532, NMC622, NMC71515, NMC811, that stored excessive two-layer Li, as shown in Figure S7. In this two-layer Li storage scenario, the oxygen ions have a face-centered cubic close-packing arrangement, which is consistent with a normal one-layer Li storage structure. All the transition metal ions take the octahedral interstitial as normal, and there are no more octahedral interstitial accommodated double Li ions between the two transition slabs. Therefore, all the Li ions occupy the tetrahedral interstitial sites which are exactly twice as much as that of octahedral interstitial sites. Thus, the chemical formula of pre-lithiated NMC can be taken to be Li_2MO_2 (M = Ni, Mn, Co). Compared with the normal $LiMO_2$, the lattice parameter *c* along the layer orientation of Li_2MO_2 is increased about 10%. This is in good agreement with the XRD detection of a new peak NMC (001) close to the (003) peak (Figure 5c).[7,15] Then, the average delithiation potentials of the excess Li storage for this pre-lithiation NMC group were calculated, based on the classic equation[20]

$$V = -\left\{\frac{E(\mathrm{Li}_{x+\Delta x}\mathrm{R}) - E(\mathrm{Li}_x\mathrm{R})}{\mathrm{d}x} - E(\mathrm{Li})\right\}$$

where $E(\mathrm{Li}_x\mathrm{MO}_2)$ and $E(\mathrm{Li}_{x+\delta x}\mathrm{MO}_2)$ stand for the total energy before and after δx lithium ions are removed from the unit formula Li_2MO_2 compound, and $E(\mathrm{Li})$ is the total chemical potential of lithium metal. The calculated results are shown in Figure 6; the delithiation voltages of NMC532, 622, 71515, 811 are 1.66, 1.96, 2.01, and 2.11 V, respectively, very close to the experimental initial charge voltages of 1.68, 1.90, and 1.98 V as shown in Figure 2b. The potentials of lithiation that push the extra Li ions to the normal single lithium layer of this group NMC were also calculated. The calculated results are about 0.91 V for these pre-lithiated NMC. The calculated values are lower than experimental values, because the only consideration is the thermodynamical perspective, while the kinetic progress whereby the diffusion of Li ions to inner tetrahedral sites must

DOI: 10.1021/acsami.6b03730
ACS Appl. Mater. Interfaces 2016, 8, 15361−15368

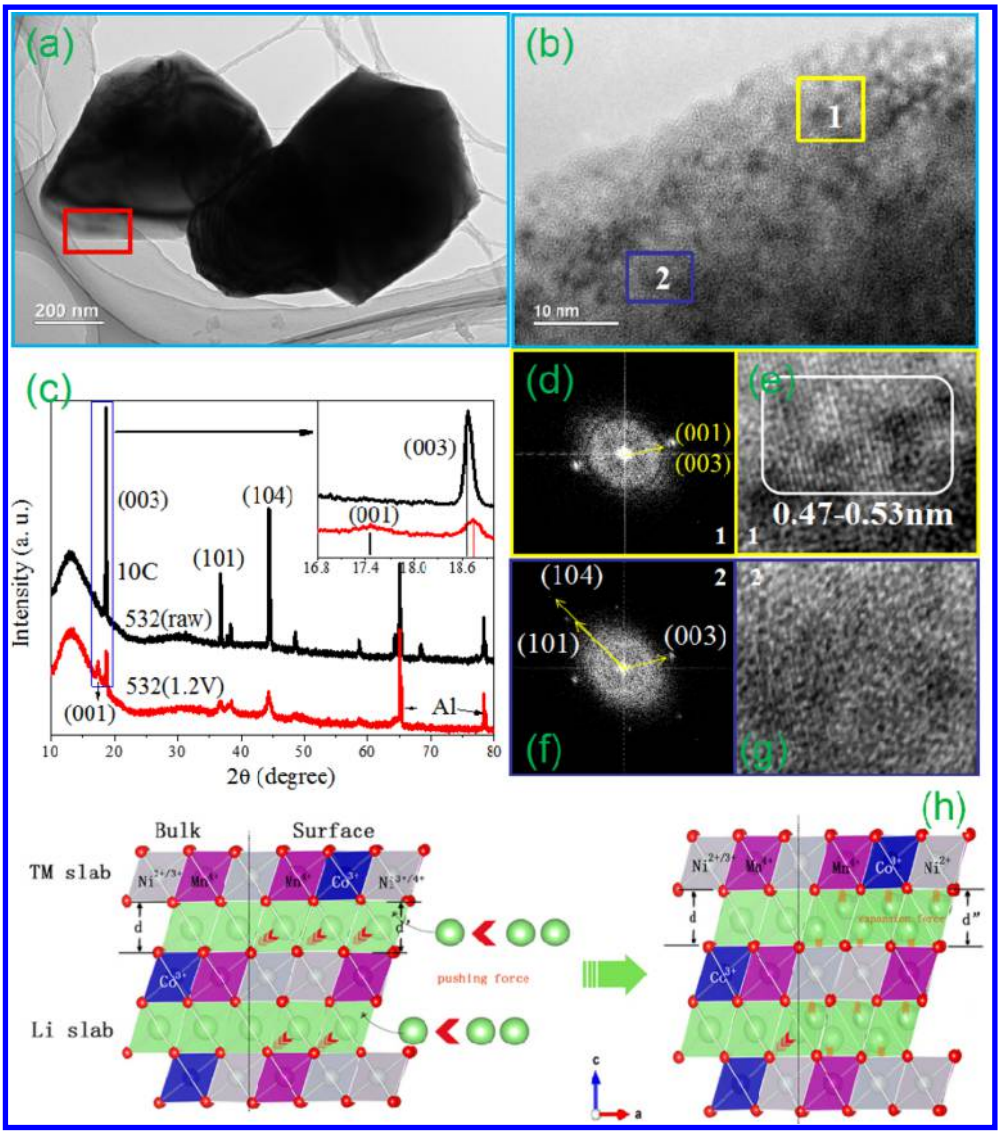

Figure 5. TEM and XRD characterizations of the morphology and structure of the NMC532 particles after pre-lithiation: (a) TEM images, (b) magnified view of the selected areas as labeled by the red square in (a), (c) XRD patterns before and after pre-lithiation, (d,e,f,g) electron diffraction and high-resolution images of point 1 and 2 in (b), and (h) the schematic mechanics of pre-lithiation process for high nickel NMC.

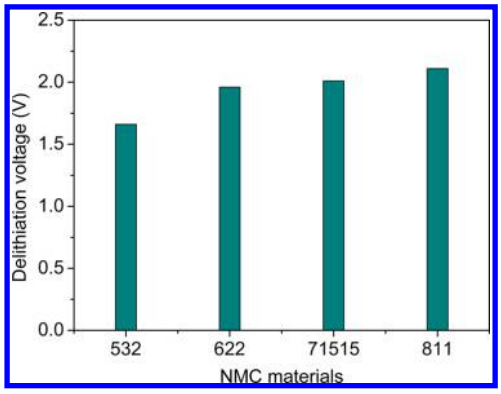

Figure 6. Upper potential limit for the reduction of Ni in the NMC serial materials in the pre-lithiation.

pass octahedral sites by pushing occupied octahedral Li to adjacent tetrahedral sites is neglected.[21,22] The intercalation schematic is shown in Figure 5h. For the pre-lithiated sample, all Ni^{3+} will be reduced to Ni^{2+} during the lithiation process, while the Li layer is eventually loaded with two slabs of Li ions.

Given the excess capacities brought by the double Li-layer structure, its thermal stability is also studied, as shown in Figure 7. The in situ XRD experiments are conducted during a thermal cycle between room temperature and 440 °C. With the increase of the temperature, the intensity of the (001) peak decreases gradually until disappearing as the temperature ramps up to 400 °C. The (001) peak will not emerge again as the sample cools down, indicating that the double-layered Li structure is not thermally stable and the irreversible decomposition will happen at elevated temperature. However, given the fact that most nonaqueous electrolytes in Li-ion batteries cannot survive temperatures higher than 100 °C, and that the polyolefin-based separators would fail below 160 °C,[23] this thermal instability of double Li layer structure, which seems to withstand temperatures up to 320 °C, does not constitute a limiting factor to the high temperature applications of the corresponding NMC materials.

DOI: 10.1021/acsami.6b03730
ACS Appl. Mater. Interfaces 2016, 8, 15361−15368

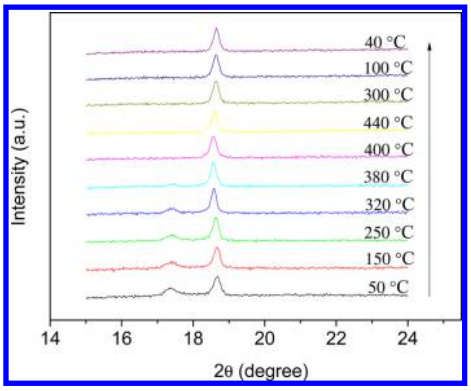

Figure 7. XRD patterns of the NMC532 materials after pre-lithiation in a thermal cycle between room temperature and 440 °C.

For further comparison, the cycling performances of two representative NMC materials (NMC442 and NMC532) selected from these two distinct NMC groups are studied, with or without pre-lithiation, at the charging/discharging rate of 2 C and 5 C as shown in Figure 8, while their pre-lithiation potentials are also optimized by applying varying cutoff potentials. The original discharge capacities for both NMC materials in the first cycle are about 150 mAh/g. Pre-lithiation improves both capacity utilization as well as capacity retention, and there seems to be an optimized lithiation voltage at all the charging/discharging rates. When the NMC material is pre-lithiated below this optimized value, the performance deteriorates. However, compared with the Ni^{3+} free NMC442 material, NMC532 obviously outperforms in both capacity utilization and capacity retention. The most conspicuous improvements occur when the charging/discharging rate is 5 C, where the capacity of NMC532 without pre-lithiation is nearly zero because of the significant polarization at high charging/discharging rate. However, pre-lithiation at the optimized voltage of 1.53 V increases the capacity to 158 mAh/g and retains it during long cycling times. All these electrochemical performances are consistent with our hypothesis based on the critical role of Ni^{3+} during the pre-lithiation.

While the excess capacity released at potential above 3.0 V can be attributed to the Ni^{3+} content in NMC materials, the improved cycling stability observed on all the NMC materials should arise from the protective interphase formed during the pre-lithiation process as discussed in our previous work.[7] For the samples prepared by slurry method in this paper, the interphase can also be discovered on both NMC442 and NMC532 as shown in Figure 9. New peaks appear in the FTIR data of the NMC materials even as early as 1.7 V, higher than the beginning of the pre-lithiation, and the peak intensities increase with the decreasing cell potential. Similar conclusion can be obtained from XPS (Figures S8 and S9). With the increasing depth of lithiation, the amounts of Li and F elements increase and the contents of Ni, Mn, and Co decrease until they completely disappear, indicating that the protective interphase layer mainly consists of decomposition products from the organic electrolytes on the surfaces of both NMC442 and NMC532 particles. Such an interphase has been believed to be effective in preventing dissolution of Mn.

CONCLUSIONS

In conclusion, we conducted a systematic study on how pre-lithiation affects the electrochemical properties of NMC materials prepared by conventional slurry approach and identified what structural unit in NMC is responsible for the excess Li storage capacity by experimental investigation and ab initio calculations. Interestingly, during pre-lithiation by low voltages to about 1.5 V, Li ions can occupy from the single octahedral layer to the tetrahedral interstitial sites for those NMCs containing Ni^{3+} (such as NMC532, 622, 71515) leading to twice as many Li ions stored. We found that desired solid

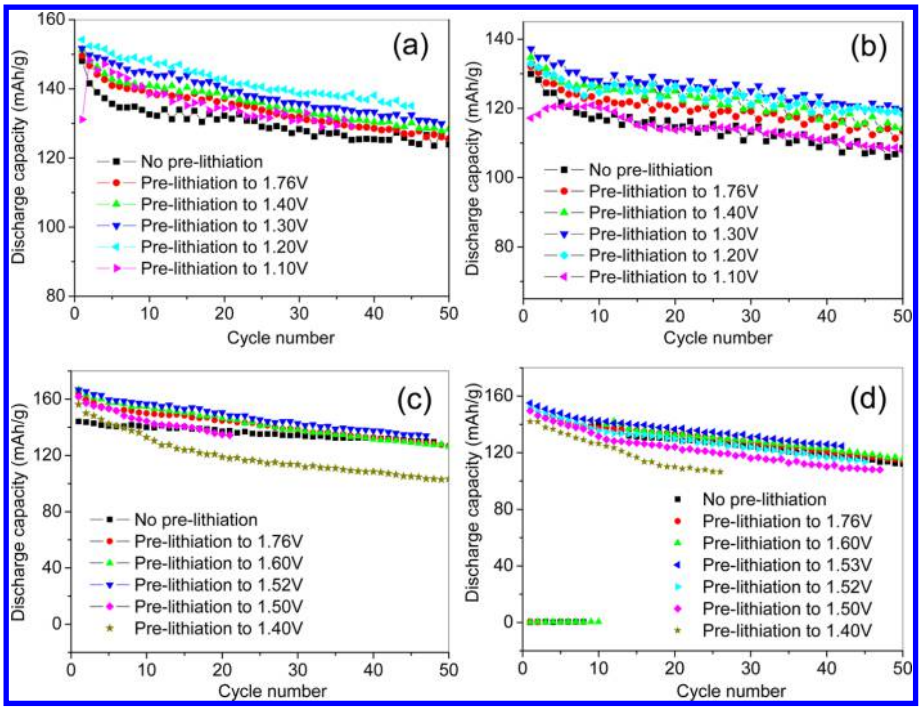

Figure 8. Cycling performances of NMC442 and NMC532 at high charging/discharging rate: (a) NMC442−2C, (b) NMC442−5C, (c) NMC532−2C, and (d) NMC532−5C.

DOI: 10.1021/acsami.6b03730
ACS Appl. Mater. Interfaces 2016, 8, 15361−15368

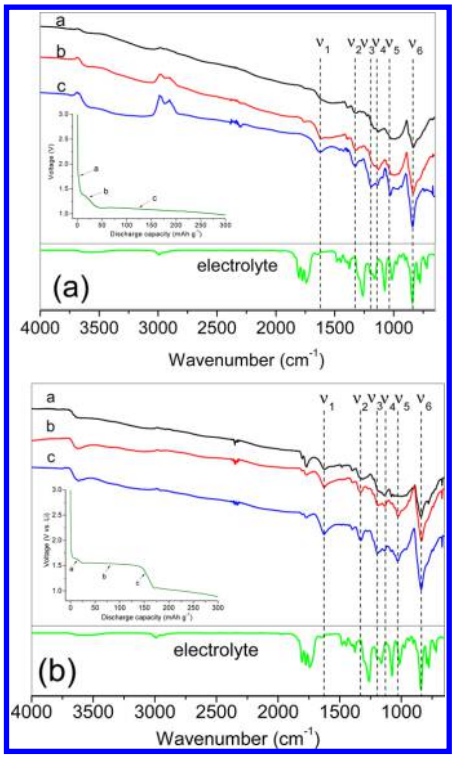

Figure 9. FTIR of $Li(Ni_{0.42}Mn_{0.42}Co_{0.16})O_2$ and $Li(Ni_{0.5}Mn_{0.3}Co_{0.2})O_2$ at different charging/discharging states showed in the insets: (a) NMC442, (b) NMC532.

electrolyte interphase (SEI) and significant depolarization were brought about by pre-lithiation onto those NMC materials in a similar manner to NMC/CNT composite materials prepared by filtration approach. More importantly, the cycling performance and reversible capacities of these NMC materials are improved significantly at the high charging/discharging rates. According to the efficiency of pre-lithiation and the consequent electrochemical behaviors, NMC materials can be divided into two distinctly different groups, the origin of which lies in the Ni-content and their valence. NMC materials that contains Ni^{3+} could be easily activated by pre-lithiation and accommodate the insertion of double-layered Li substructure, while those Ni^{3+}-free NMC materials cannot be activated at potential above 1.0 V for excess Li insertion, characterized by the limited improvements in their electrochemical performance. The double-layered Li structure emerges at certain locations of the Ni^{3+}-containing NMC particles during the pre-lithiation and the consequent reduction from Ni^{3+} to Ni^{2+}, and this substructure remains stable up to 320 °C. Such a Li-rich substructure provides potential excess capacity for the cathode materials based on NMC lattices.

■ ASSOCIATED CONTENT

Supporting Information

The Supporting Information is available free of charge on the ACS Publications website at DOI: 10.1021/acsami.6b03730.

SEM morphology of NMC; XRD patterns of NMC71515, 622, 552, 442, 111 at different charge/discharge states; calculated structures for pre-lithiation; XPS of NMC532, 442 at different charge/discharge states (PDF)

■ AUTHOR INFORMATION

Corresponding Author

*E-mail: panfeng@pkusz.edu.cn. Tel: 86-755-26033200.

Author Contributions

#Zhongzhen Wu, Shunping Ji, and Zongxiang Hu contributed equally.

Notes

The authors declare no competing financial interest.

■ ACKNOWLEDGMENTS

This work was financially supported jointly by National Science Foundation of China (No. 51301004), Guangdong Innovation Team Project (No. 2013N080), Shenzhen Peacock Plan (Grant No. KYPT20141016105435850), and Shenzhen Science and Technology Research Grant (No. JCYJ20140903102215536, JCYJ20150828093127698 and ZDSY20130331145131323).

■ REFERENCES

(1) Uchaker, E.; Cao, G. Mesocrystals as Electrode Materials for Lithium-Ion Batteries. *Nano Today* **2014**, *9*, 499−524.

(2) Tarascon, J. M.; Armand, M. Issues and Challenges Facing Rechargeable Lithium Batteries. *Nature* **2001**, *414*, 359−367.

(3) Zhan, C.; Lu, J.; Kropf, A. J.; Wu, T.; Jansen, A. N.; Sun, Y.-K.; Qiu, X.; Amine, K. Mn(II) Deposition on Anodes and Its Effects on Capacity Fade in Spinel Lithium Manganate-Carbon Systems. *Nat. Commun.* **2013**, *4*, 2437.

(4) Wang, L.; Li, J.; He, X.; Pu, W.; Wan, C.; Jiang, C. Recent Advances in Layered $LiNi_xCo_yMn_{1-x-y}O_2$ Cathode Materials for Lithium Ion Batteries. *J. Solid State Electrochem.* **2009**, *13*, 1157−1164.

(5) Lin, F.; Markus, I. M.; Nordlund, D.; Weng, T.-C.; Asta, M. D.; Xin, H. L.; Doeff, M. M. Surface Reconstruction and Chemical Evolution of Stoichiometric Layered Cathode Materials for Lithium-Ion Batteries. *Nat. Commun.* **2014**, *5*, 3529.

(6) Wu, Z.; Han, X.; Zheng, J.; Wei, Y.; Qiao, R.; Shen, F.; Dai, J.; Hu, L.; Xu, K.; Lin, Y.; Yang, W.; Pan, F. Depolarized and Fully Active Cathode Based on $Li(Ni_{0.5}Co_{0.2}Mn_{0.3})O_2$ Embedded in Carbon Nanotube Network for Advanced Batteries. *Nano Lett.* **2014**, *14*, 4700−4706.

(7) Wu, Z.; Ji, S.; Zheng, J.; Hu, Z.; Xiao, S.; Wei, Y.; Zhuo, Z.; Lin, Y.; Yang, W.; Xu, K.; Amine, K.; Pan, F. pre-lithiation Activates $Li(Ni_{0.5}Co_{0.2}Mn_{0.3})O_2$ for High Capacity and Excellent Cycling Stability. *Nano Lett.* **2015**, *15*, 5590−5596.

(8) Blöchl, P. E. Projector Augmented-Wave Method. *Phys. Rev. B: Condens. Matter Mater. Phys.* **1994**, *50*, 17953−17979.

(9) Kresse, G.; Joubert, D. From Ultrasoft Pseudopotentials to the Projector Augmented-Wave Method. *Phys. Rev. B: Condens. Matter Mater. Phys.* **1999**, *59*, 1758−1775.

(10) Kresse, G.; Furthmüller, J. Efficient Iterative Schemes for Ab Initio Total-Energy Calculations Using a Plane-Wave Basis Set. *Phys. Rev. B: Condens. Matter Mater. Phys.* **1996**, *54*, 11169−11186.

(11) Kresse, G.; Furthmüller, J. Efficiency of Ab-Initio Total Energy Calculations For Metals and Semiconductors Using a Plane-Wave Basis Set. *Comput. Mater. Sci.* **1996**, *6*, 15−50.

(12) Perdew, J. P.; Burke, K.; Ernzerhof, M. Generalized Gradient Approximation Made Simple. *Phys. Rev. Lett.* **1996**, *77*, 3865−3868.

(13) Anisimov, V. I.; Zaanen, J.; Andersen, O. K. Band theory and Mott insulators: Hubbard U instead of Stoner I. *Phys. Rev. B: Condens. Matter Mater. Phys.* **1991**, *44*, 943−954.

(14) Kang, S.-H.; Park, S.-H.; Johnson, C. S.; Amine, K. Effects of Li Content on Structure and Electrochemical Properties of $Li_{1+x}(Ni_{0.5}Mn_{0.5})_{1-x}O_2$ ($0 \leq x \leq 0.15$) Electrodes in Lithium Cells (1.0−4.8 V). *J. Electrochem. Soc.* **2007**, *154*, A268−A274.

(15) Johnson, C. S.; Kim, J.-S.; Kropf, A. J.; Kahaian, A. J.; Vaughey, J. T.; Fransson, L. M. L.; Edstrom, K.; Thackeray, M. M. Structural Characterization of Layered $Li_xNi_{0.5}Mn_{0.5}O_2$ ($0 < x \leq 2$) Oxide Electrodes for Li Batteries. *Chem. Mater.* **2003**, *15*, 2313−2322.

DOI: 10.1021/acsami.6b03730
ACS Appl. Mater. Interfaces 2016, 8, 15361−15368

(16) Zhang, L.; Li, N.; Wu, B.; Xu, H.; Wang, L.; Yang, X.; Wu, F. Sphere-Shaped Hierarchical Cathode with Enhanced Growth of Nanocrystal Planes for High-Rate and Cycling-Stable Li-Ion Batteries. *Nano Lett.* **2015**, *15*, 656−661.
(17) Cho, Y.; Oh, P.; Cho, J. A New Type of Protective Surface Layer for High-Capacity Ni-Based Cathode Materials: Nanoscaled Surface Pillaring Layer. *Nano Lett.* **2013**, *13*, 1145−1152.
(18) Yang, X.-Q.; McBreen, J.; Yoon, W. S.; Grey, C. P. Crystal Structure Changes of $LiMn_{0.5}Ni_{0.5}O_2$ Cathode Materials During Charge and Discharge Studied by Synchrotron Based in Situ XRD. *Electrochem. Commun.* **2002**, *4*, 649−654.
(19) Kosova, N. V.; Devyatkina, E. T.; Kaichev, V. V. Optimization of Ni^{2+}/Ni^{3+} Ratio in Layered Li(Ni, Mn, Co)O_2 Cathodes for Better Electrochemistry. *J. Power Sources* **2007**, *174*, 965−969.
(20) Ceder, G.; Ven, A. V.; Marianetti, C.; Morgan, D. First-Principles Alloy Theory in Oxides. *Modell. Simul. Mater. Sci. Eng.* **2000**, *8*, 311−321.
(21) Van der Ven, A.; Ceder, G. Lithium Diffusion Mechanisms in Layered Intercalation Compounds. *J. Power Sources* **2001**, *97*−*98*, 529−531.
(22) Morgan, D.; Van der Ven, A.; Ceder, G. Li Conductivity in Li_xMPO_4 (M = Mn, Fe, Co, Ni) Olivine Materials. *Electrochem. Solid-State Lett.* **2004**, *7*, A30−A32.
(23) Xu, K. Nonaqueous Liquid Electrolytes for Lithium-Based Rechargeable Batteries. *Chem. Rev.* **2004**, *104*, 4303−4417.

DOI: 10.1021/acsami.6b03730
ACS Appl. Mater. Interfaces 2016, 8, 15361−15368